*R*esearch in
*A*stronomy and
*A*strophysics

EDITOR'S RECOMMENDATION

The NGC 7742 star cluster luminosity function: a population analysis revisited

Richard de Grijs[1,2,3] and Chao Ma[1,2]

[1] Kavli Institute for Astronomy & Astrophysics, Peking University, Beijing 100871, China; *grijs@pku.edu.cn*
[2] Department of Astronomy, Peking University, Beijing 100871, China
[3] International Space Science Institute–Beijing, Beijing 100190, China

Abstract We re-examine the properties of the star cluster population in the circumnuclear starburst ring in the face-on spiral galaxy NGC 7742, whose young cluster mass function has been reported to exhibit significant deviations from the canonical power law. We base our reassessment on the clusters' luminosities (an observational quantity) rather than their masses (a derived quantity), and confirm conclusively that the galaxy's starburst-ring clusters—and particularly the youngest subsample, $\log(t\,\mathrm{yr}^{-1}) \leq 7.2$— show evidence of a turnover in the cluster luminosity function well above the 90% completeness limit adopted to ensure the reliability of our results. This confirmation emphasizes the unique conundrum posed by this unusual cluster population.

Key words: globular clusters: general — galaxies: evolution — galaxies: individual (NGC 7742) — galaxies: star clusters: general — galaxies: star formation

1 RAPID STAR CLUSTER EVOLUTION

Until recently, neither theoretical predictions nor prior observational evidence indicated that the power-law cluster luminosity functions (CLFs) and the equivalent cluster mass functions (CMFs) commonly found for very young star cluster systems could transform into the log-normal distributions characteristic of old globular clusters on timescales as short as a few $\times 10^7$ yr. Yet, preliminary evidence is emerging of enhanced cluster disruption on very short timescales in the complex galactic dynamical environments of circumnuclear starburst rings (for a brief review, see de Grijs et al. 2017).

Over the past few decades, significant efforts have been expended to understand the process of star cluster disruption (e.g., Boutloukos & Lamers 2003; Gieles et al. 2005; Lamers et al. 2005; Baumgardt et al. 2008; Fall et al. 2009; Vesperini et al. 2009). Mengel et al. (2005) sorted the various disruptive processes acting on star clusters into a number of different types, as a function of cluster age. Following an initial period of rapid

supernova-driven cluster expansion and dissolution of up to a few $\times 10^7$ yr, cluster disruption is predominantly driven by internal two-body relaxation processes and stellar evolution, at least in the absence of significant external perturbations (which is, however, unlikely to be the case in the dense and dynamically complex environments of starburst rings). In turn, in quiescent environments the initial power-law CLFs and CMFs transform into the well-established bell-shaped distributions characteristic of old globular clusters on timescales of billions of years.

The discovery by de Grijs & Anders (2012) of a lognormal-like CMF for star clusters as young as ~ 10 Myr in the circumnuclear starburst ring galaxy NGC 7742 was therefore unexpected. de Grijs & Anders (2012) argued that, except if one releases the assumption that the initial CMF was a power law—which would contradict most observational studies in this very active area of current research—three effects could potentially have caused this discrepancy: (i) technical issues

related to the cluster age and mass determinations, (ii) evolution of the star cluster population on very short timescales ($\lesssim 10^7$ yr), and/or (iii) differences in the cluster formation conditions compared with other environments known to host large samples of young star clusters. They ruled out an origin related to their analysis approach (i.e., option i) based on a careful technical assessment.

The community's commonly accepted point of view has gradually evolved to embrace the idea that star clusters form following a power-law CMF. This power-law form seems indeed ubiquitous and appears to be independent of the initial stellar and gas densities. Therefore, an initial power-law CMF seemed a reasonable, physically motivated boundary condition for the observed CMF in NGC 7742, and one can thus rule out option (iii) above (for detailed arguments, see de Grijs & Anders 2012). This leaves us with option (ii) as the most likely origin of the observed peaked CMF. This initial conclusion was strengthened by the recent study of Väisänen et al. (2014), who discovered similar evidence of rapid star cluster disruption in the early-type galaxy NGC 2328.

2 CLUSTER MASS VERSUS LUMINOSITY FUNCTIONS

However, we have long been concerned about the high mass at which the peak of the apparent CMF turnover in NGC 7742 seems to occur,

$$\log(M_{\rm cl}/M_\odot) \approx 5.6.$$

Our concerns were fanned by similar criticism voiced by other active scientists in the field, which—as we will see in this paper—was indeed justified to some extent. We therefore decided to re-analyze the NGC 7742 cluster population by focusing exclusively on its *luminosity* function as the most straightforward diagnostic tool that does not require one to adopt the kind of assumptions needed to derive cluster masses. We proceeded entirely independently from our earlier work (the data re-reduction was performed independently as well), to the extent that we even downloaded the latest pipeline-processed *Hubble Space Telescope* (*HST*) images from the Hubble Legacy Archive.[1] The data reduction procedures employed followed the same general approach as those adopted by de Grijs et al. (2013, 2017).

---

[1] *http://hla.stsci.edu/hlaview.html*

2.1 Completeness Analysis

In the context of our CLF shape analysis, it is crucial to understand how many objects may have been missed in a statistical sense by our processing technique. We employed our previously well-established approach to determine the extended cluster sample's incompleteness (e.g., de Grijs et al. 2017; and references therein), of which we summarize the salient features here. We first applied the IRAF tasks STARLIST and MKOBJ to generate 500 artificial sources with FWHM = 1.7, 2.6 and 3.4 pixels, corresponding to approximately 19, 29 and 37 pc, respectively, at the distance of NGC 7742, $D = 22.2$ Mpc. These sizes represent true point sources and objects with the sample's median and mean sizes, respectively. Two-thirds of our sample objects have sizes smaller than the mean size; any larger objects are confirmed cluster complexes. We chose to use 10 runs of 500 artificial objects each to minimize the effects of crowding and blending, both between artificial sources and between artificial and real objects. We checked and confirmed that using 800 sources or more did not change the final completeness results. We also checked, specifically for the point-source tests, that using realistic WFPC2 point-spread functions instead of Gaussian point sources did not lead to statistically significant changes to the results. Finally, both authors performed the completeness analysis independently to cross check the reliability of the results.

We sampled our artificial objects at random (X, Y) coordinates, ensuring that they were easily identifiable as single sources (that is, they were not affected by either crowding or blending); 260 of the 500 input sources were located in the ring region defined by de Grijs & Anders (2012):

$$50 \leq R \leq 125 \quad \text{pixels}.$$

Next, we generated a blank template image without any background noise and of the same size as that of the actual NGC 7742 field of view considered here. We then added the artificial sources located in the ring region to the template image. All artificial objects were assigned the same magnitude; we repeated this process by varying the magnitudes of the input sources from 19.0 mag to 27.0 mag in both the F555W and F814W filters (roughly equivalent to the Johnson–Cousins V and I broad-band filters), in steps of 0.5 mag.

Finally, we re-'discovered' (and re-measured) the number of artificial sources in both the template and science images, using the same approach for both. (We
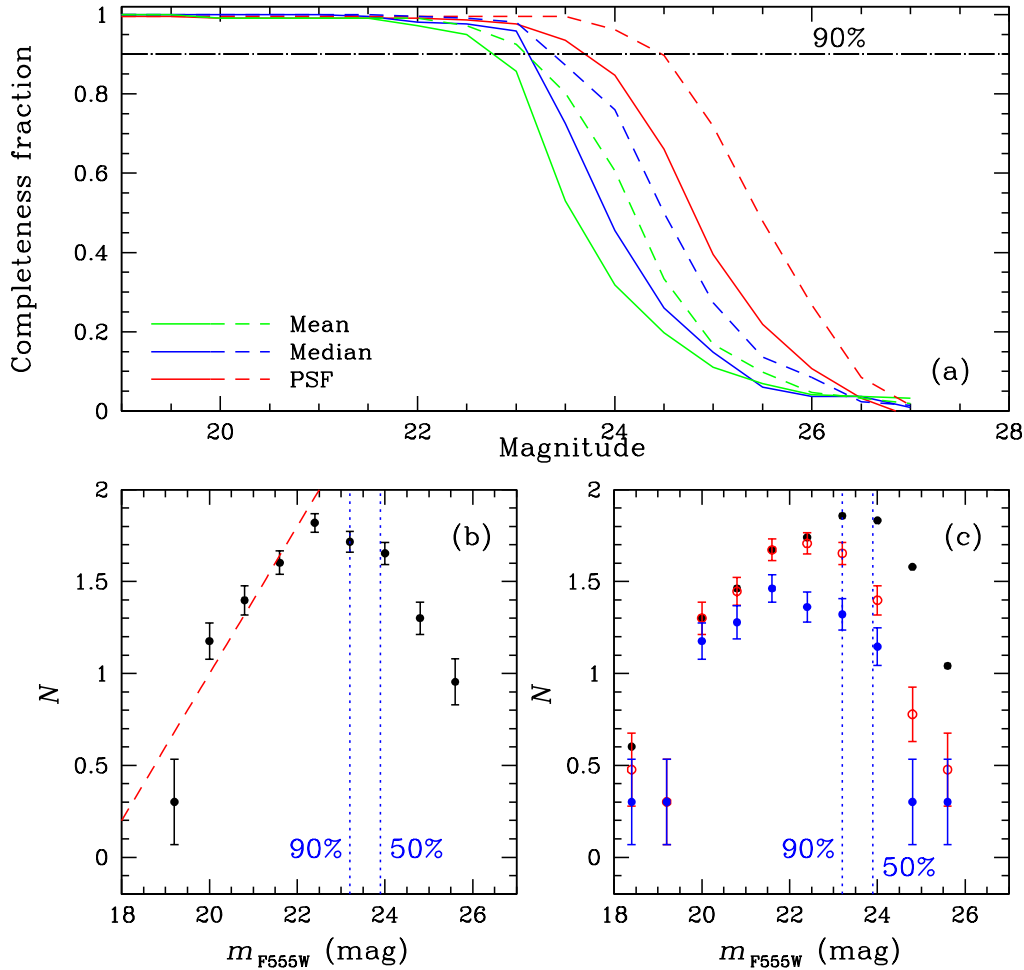
Fig. 1 NGC 7742 re-analysis. (a) Completeness fractions for point sources ('PSF'), median and mean sizes (FWHM = 1.7, 2.2 and 2.6 pixels, respectively) in the NGC 7742 starburst ring, at galactocentric radii $0.52 \leq R \leq 1.35$ kpc (corresponding to the ring region adopted by de Grijs & Anders 2012) in the F555W (*solid lines*) and F814W (*dashed lines*) filters used for the initial source selection and spatial cross correlation. (b) CLF of the full sample of starburst-ring clusters, based on a complete re-analysis of the NGC 7742 data sets. The 50% and 90% completeness limits in the limiting filter (F555W) for clusters of median size pertaining to the starburst ring area are shown as vertical blue dotted lines; the canonical $\alpha = 2$ power-law CLF is represented by the red dashed line. (c) As panel (b) but for the original data analyzed by de Grijs & Anders (2012), adjusted for the zero-point difference derived in our re-analysis (see the text). The black data points represent the CLF of the entire cluster population (uncertainties are not included for reasons of clarity), while the red CLF relates to the ring's subsample. The blue CLF shows the distribution of clusters with ages $\log(t \text{ yr}^{-1}) \leq 7.2$.

applied our source discovery routine to the science images to find the real clusters using the exact same approach.) Since the template image contained no background noise, we can recover most input artificial sources to within the associated measurement uncertainties, although some may have disappeared into the physical

noise of the science images, depending on the combinations of their integrated magnitudes and extent, as well as on the presence of real background variations. In addition, saturated sources and blending may cause failures to recover the artificial sources. The template image hence became a perfect comparison sample to check how many

sources should be recovered under ideal conditions. By redetermining the photometric and structural properties (i.e., the Gaussian sizes) of the artificial sources in the combined science and template images as a function of input magnitude, we get a quantitative handle on the effects of background noise. We counted the number of recovered artificial sources with magnitudes and Gaussian σ's within the 1σ uncertainties of the input magnitudes (from the science+template image) and the number of recovered artificial sources of the same photometric quality and with similar sizes (from the template) to estimate the completeness, i.e.

$$f_{\rm comp} = N_{\rm rec}/N_{\rm tot},$$

where $N_{\rm rec}$ is the number of artificial objects we recovered and $N_{\rm tot}$ is the number of input objects.

Our approach ensured that $f_{\rm comp}$ was simultaneously corrected for the effects of blending and saturation, as well as background noise. Since our artificial sources are extended objects, correcting for the effects of crowding and blending is important. We corrected for and removed blends of artificial sources.

Figure 1(a) shows the completeness curves in the starburst ring area for sources with sizes equivalent to the PSF, median and mean cluster sizes in the F555W and F814W images, which were initially used for our selection of genuine sources and their spatial cross correlation. This panel indicates that the F555W filter is our limiting passband. In our recent papers (e.g., de Grijs et al. 2017; and references therein) we have adopted the 90% completeness level as our threshold for source detections to underscore the robustness of our results. These levels occur at ~ 0.5–1.0 mag brighter magnitudes than the conventionally used 50% completeness limits, in all filters. The 90% completeness limit in the NGC 7742 ring area is reached at F555W magnitudes of $m_{\rm F555W} = 23.7, 23.2$ and 22.8 mag for point sources and objects with the cluster population's median and mean sizes, respectively.

Our independent approach uncovered 280 cluster candidates associated with the galaxy's starburst ring, a number that is sufficiently close to the 256 ring clusters identified by de Grijs & Anders (2012) to confirm our confidence in the earlier sample selection. The full ring CLF is shown in Figure 1(b), where we have also indicated the 50% and 90% completeness levels and the expected, canonical $\alpha = 2$ power-law CLF for a single-aged cluster population shortly after cluster formation. We point out that this latter condition is not met by the

full cluster population in the NGC 7742 starburst ring (de Grijs & Anders 2012; their fig. 1). We show the canonical power-law CLF simply for guidance.

2.2 Direct Comparison with Earlier Results

A direct comparison of the F555W CLF in Figure 1(b) with the CLF underlying the data presented by de Grijs & Anders (2012) raised an immediate concern: while the *shapes* of both CLFs were similar, the *luminosities* of the main features differed significantly, in the sense that the turnover in the newly derived CLF occurred at a ~ 2.1 mag fainter level (when compared with the peak in the CMF, expressed in magnitudes, by adopting a suitable age-dependent mass-to-light ratio). Careful examination of the potential cause(s) of this difference revealed that the image header keywords PHOTFLAM adopted in de Grijs & Anders (2012) were incorrectly populated in the original *HST* data frames (STScI n.d.[2]). We hence adjusted our original photometry following the *HST* project team's recommendations, resulting in the CLFs shown in 1(c).

Figure 1(c) shows the full NGC 7742 CLF (black), as well as the CLF for the starburst ring only (red), where we used the same radial range as de Grijs & Anders (2012) to define the ring region, i.e.,

$$0.52 \le R \le 1.35 \text{ kpc}.$$

The latter CLF is appropriate for comparison with the CLF shown in Figure 1(b). Within the statistical uncertainties, both CLFs are indeed similar. Our cluster sample exhibits a clear although broad luminosity–size relation (not shown), in the sense that more extended objects tend to be brighter. Therefore, even if we somehow missed a sizeable number of more extended sources, it is unlikely this would explain the observed turnover, given that such extended sources would be missed at the bright end of the distribution. In view of the available observational evidence, we therefore conclude that the observed turnover in the CLF is real and not owing to technical aspects associated with our data reduction approach.

Unfortunately, our NGC 7742 data set does not include Hα images, which would have allowed us to independently confirm the clusters' young ages, as we did in de Grijs et al. (2017) for a number of other young

---

[2] STScI, n.d., WFPC2 Advisory: Incorrect PHOTFLAM header keyword value in Multidrizzle output images. *http://www.stsci.edu/hst/wfpc2/documents/photflam.pdf*

starburst ring CLFs. Therefore, we used the cluster ages derived by de Grijs & Anders (2012) to make a further selection of the youngest clusters only. Following de Grijs & Anders (2012), we selected all clusters with ages $\log(t \text{ yr}^{-1}) \leq 7.2$ as representative of the youngest CLF. The latter is shown as the blue CLF.

3 VERDICT

Keeping in mind that our age estimates are based on broad-band spectral-energy distributions composed of only four filters (which hence implies that they are affected by significant uncertainties; see de Grijs & Anders 2012), it is clear that the 90% completeness limit occurs at a brightness level that is at least 1 mag fainter than the onset of the apparent turnover. It thus appears that while our mass estimates were rendered too high by the incorrectly populated *HST* header keywords, the *shape* of the young CLF resembles that of the young cluster *mass* function. Despite our more thorough analysis presented here, we have thus been unable to discredit our earlier analysis of the NGC 7742 CMF beyond a reasonable doubt. The galaxy's young ring CLF and CMF indeed exhibit clear and robust turnovers that are unexpected from standard cluster evolution theory.

We have compiled a catalog of well-resolved nuclear rings that have been observed with both the *HST* in at least four filters (ideal for our star cluster analysis) and the *Spitzer Space Telescope* (see Ma et al. 2017). NGC 7742 is an outlier in our ring catalog. Traditional nuclear rings are formed as the result of bar-driven gas inflows, which makes them resemble two winded spirals; their host galaxies are usually barred spirals (see, e.g., NGC 1512 and NGC 6951; de Grijs et al. 2017) and their CLFs (CMFs) do not exhibit any obvious turnovers. However, the circumnuclear starburst ring in NGC 7742 (an unbarred face-on spiral galaxy), although similar in size to the rings in other ring galaxies, is almost fully circular and highly symmetric.

The mass of the circumnuclear ring in NGC 7742, $M_{\text{ring}} \sim 6 \times 10^9 M_\odot$, is large with respect to the stellar mass of the galaxy as a whole, $M_{\text{gal}} \sim 5.9 \times 10^{10} M_\odot$ (C. Ma et al., in prep.). The latter value is based on the galaxy's mass-to-light ratio published by Bell et al. (2003) and its integrated K-band magnitude from Huchra et al. (2012); we determined the ring mass following the same approach as Ma et al. (2017). An origin related to a minor merger event has been proposed

as an alternative to the bar-driven gas flows usually invoked (Sil'chenko & Moiseev 2006; see also Mazzuca et al. 2006; Tutukov & Fedorova 2006). Further investigation of a larger sample of ring galaxies will be required to shed conclusive light onto the processes driving the establishment of the unusual type of young CLF (CMF) first uncovered in NGC 7742. A partial reassessment of our current understanding of the star cluster evolution scenario may well be on the cards.

References

Baumgardt, H., Kroupa, P., & Parmentier, G. 2008, MNRAS, 384, 1231

Bell, E. F., McIntosh, D. H., Katz, N., & Weinberg, M. D. 2003, ApJS, 149, 289

Boutloukos, S. G., & Lamers, H. J. G. L. M. 2003, MNRAS, 338, 717

de Grijs, R., & Anders, P. 2012, ApJ, 758, L22

de Grijs, R., Anders, P., Zackrisson, E., & Östlin, G. 2013, MNRAS, 431, 2917

de Grijs, R., Ma, C., Jia, S., Ho, L. C., & Anders, P. 2017, MNRAS, 465, 2820

Fall, S. M., Chandar, R., & Whitmore, B. C. 2009, ApJ, 704, 453

Gieles, M., Bastian, N., Lamers, H. J. G. L. M., & Mout, J. N. 2005, A&A, 441, 949

Huchra, J. P., Macri, L. M., Masters, K. L., et al. 2012, ApJS, 199, 26

Lamers, H. J. G. L. M., Gieles, M., & Portegies Zwart, S. F. 2005, A&A, 429, 173

Ma, C., de Grijs, R., & Ho, L. C. 2017, ApJS, 230, 14

Mazzuca, L. M., Sarzi, M., Knapen, J. H., Veilleux, S., & Swaters, R. 2006, ApJ, 649, L79

Mengel, S., Lehnert, M. D., Thatte, N., & Genzel, R. 2005, A&A, 443, 41

Sil'chenko, O. K., & Moiseev, A. V. 2006, AJ, 131, 1336

Tutukov, A. V., & Fedorova, A. V. 2006, Astronomy Reports, 50, 785

Väisänen, P., Barway, S., & Randriamanakoto, Z. 2014, ApJ, 797, L16

Vesperini, E., McMillan, S. L. W., & Portegies Zwart, S. 2009, ApJ, 698, 615